Journal of Pharmaceutical and Biomedical Analysis 49 (2009) 715–725

Contents lists available at ScienceDirect

Journal of Pharmaceutical and Biomedical Analysis

journal homepage: www.elsevier.com/locate/jpba

Rapid identification of acetophenones in two *Cynanchum* species using liquid chromatography–electrospray ionization tandem mass spectrometry

Xi Zhang[a,1], Lei Shan[a,1], Hao Huang[b], Xianwen Yang[a], Xu Liang[a], Aiting Xing[a], Haiqiang Huang[a], Xinru Liu[a], Juan Su[a], Weidong Zhang[a,c,*]

[a] *Department of Natural Medicinal Chemistry, School of Pharmacy, Second Military Medical University, Shanghai 200433, PR China*
[b] *College of Pharmacy, Nankai University, Tianjin 300071, PR China*
[c] *School of Pharmacy, Shanghai Jiao Tong University, Shanghai 200030, PR China*

ARTICLE INFO

Article history:
Received 8 September 2008
Received in revised form
23 December 2008
Accepted 9 January 2009
Available online 19 January 2009

Keywords:
Acetophenone
Cynandione A derivatives
Liquid chromatography–electrospray tandem mass spectrometry
Cynanchum species
Quadrupole time-of-flight mass analyzer

ABSTRACT

Acetophenones in *Cynanchum* species, especially cynandione A and its derivatives, whose utilization and toxicity in herbal drugs and folk medicines has caused great interest in the chemical investigation, have extensive biological activities. In this paper, a facile method based on high-performance liquid chromatography coupled with electrospray ionization tandem mass spectrometry (HPLC-ESI-MS^n) was developed for the analysis of cynandione A derivatives in the roots of the *Cynanchum wilfordii* and *C. auriculatum*. ESI-MS/MS and ESI-MS^n analysis of cynandiones A and B in negative ion mode were firstly performed employing two mass spectrometers each equipped with an ion-trap and a quadrupole time-of-flight (Q-TOF) mass analyzer. The results drawn from both instruments were similar to each other. Characteristic fragmentation pathways were proposed by comparing the spectra of two standards acquired in the experiments. The fragment ions at *m*/*z* 283 and 268 were obtained, and then were used as diagnostic ions to screen and identify cynandione A derivatives from the roots of above two species, together with an HPLC-MS^n method. Total of 28 cynandione A derivatives comprising 4 reported and 24 novel components were identified or tentatively identified. Furthermore, breakdown curves were constructed to distinguish two types of isomers among these compounds. To our knowledge, this is the first report on characterization of acetophenones by HPLC-ESI-MS^n, which allows a rapid and complete analysis of cynandione A derivatives in roots of *Cynanchum* species.

1. Introduction

The genus *Cynanchum*, including about 200 species, are widespread in the world [1]. Most *Cynanchum* species have been used in folk medicines for the prevention and treatment of various types of diseases, such as curing snakebites, rheumatic arthritis and tumors. Owing to various bioactivities of *Cynanchum* species, the bioactive ingredients have been widely explored in many studies [2–4]. It was demonstrated that acetophenones, mainly cynandione A and its derivatives, had properties of hepatoprotective, neuroprotective and anti-tumor activities [2,5,6]. In view of the importance of acetophenones, it is useful to explore efficient methods to aid in the structural elucidation and characterization of these bioactive compounds from the complex extracts of *Cynanchum* species.

In the analysis of acetophenones, most efforts focused on the identification of the pure compounds isolated from *Cynanchum* species using UV, IR NMR and MS techniques [6,7–9,14]. Since the information provided by UV and IR spectroscopy is not enough to elucidate the structures of these compounds, NMR is usually used for the structural characterization of acetophenones. However, this technique requires large amounts of purified samples. Mass spectrometric techniques were used as an alternative and complementary method to NMR in natural product analysis. Although the electron ionization (EI) mass spectra and desorption chemical ionization (DCI) mass spectra of acetophenones have been reported [7,15,16], these methods only provide little structural information on purified acetophenones. Recently, high-performance liquid chromatography coupled with electrospray ionization tandem mass spectrometry (HPLC-ESI-MS/MS) presents a convenient method for the on-line identification of various natural products and biological matrix because it can provide high sensitivity and considerable structural information with relatively short analysis time and low amount of samples [10–13]. But up to now, no systematic study via HPLC-ESI-MS^n for a complete structural characterization of cynandione A and

* Corresponding author at: Second Military Medical University, No. 325 Guohe Rd., Shanghai 200433, PR China. Tel.: +86 21 25070386; fax: +86 21 25070386.
E-mail address: wdzhangy@hotmail.com (W. Zhang).
[1] These authors have the same contribution to this paper.

0731-7085/$ – see front matter © 2009 Elsevier B.V. All rights reserved.
doi:10.1016/j.jpba.2009.01.009

its derivatives from the extracts of *Cynanchum* species has been reported.

Herein, the fragmentation mechanisms of two representative acetophenones, cynandiones A and B, were investigated in detail using ESI tandem mass spectrometry equipped with an ion-trap (IT) and a quadrupole time-of-flight (Q-TOF) instruments. The fragmentation pathways and diagnostic fragment ions were obtained. On the basis of these structural information, an HPLC-ESI-MS^n method was developed for on-line identifying cynandione A derivatives in root extracts of *Cynanchum wilfordii* and *C. auriculatum* which have been used as a folk medicine (named Bai-shou-wu) in China for their anti-tumor, anti-inflammatory and anti-aging properties [1,14]. Except 4 reported, 24 compounds were presumed to be new acetophenones. Moreover, breakdown curves were constructed to discriminate isomers among these 28 substances, and the results showed that both positional isomers and chiral isomers investigated could be differentiated obviously. To our knowledge, this is the first report on the characterization of acetophenones by HPLC-ESI-MS^n, which allows a rapid, selective and sensitive for the effective analysis of cynandione A derivatives in roots of *Cynanchum* species.

2. Experimental

2.1. Chemicals and reagents

HPLC-grade acetonitrile (ACN) and methanol (MeOH) were purchased from Tedia Company Inc. (Fairfield, OH, USA). Cynandiones A and B were isolated from the roots of *C. auriculatum*. Their structures were fully identified by NMR, MS spectroscopy. Deionized water purified by a Millipore Milli-Q system (Bedford, MA, USA) was used throughout the experiment. Other solvents were of analytical grade. Standard solution of cynandiones A and B with concentration of 1 mg/mL was prepared by dissolving each sample in 80% MeOH/H_2O and stored at −20 °C for analysis.

2.2. Materials

The dried root tubers of *C. wilfordii* and *C. auriculatum* were collected from Huanren, Liaoning Province and identified by Professor Han-ming Zhang (School of Pharmacy, Second Military Medical University). Voucher specimens were deposited in Department of Pharmacognosy, Second Military Medical University.

2.3. Sample preparation procedures

The dried root tubers of *C. wilfordii* (17 kg) were ground and then extracted three times with 95% ethanol under reflux, each time for 2 h. And total of the ethanol extract was evaporated in vacuum. The residue (2 kg) was suspended in water, and then partitioned successively with petroleum ether, $CHCl_3$, EtOAc and *n*-BuOH. Part of the EtOAc extract (110.4 g) was subjected to a silica gel column chromatography (silica gel CC, 110 cm × 12 cm), gradient eluted with $CHCl_3$/MeOH (100:1,1:3, v/v) to give eight major fractions. Fraction 2 (19 g) was rechromatographed on a silica gel CC, eluting with $CHCl_3$/MeOH from the ratio of 60:1 (v/v) to 15:1 (v/v) to obtain compound **27** (53.5 mg).

The EtOAc extract of *C. auriculatum* was obtained in the same way as above-mentioned for *C. wilfordii*.

Each of the EtOAc extracts (5 g) of *C. wilfordii* and *C. auriculatum*, both contain acetophenones, was dissolved in 10 mL of methanol and passed through a 0.45 μm filter prior to HPLC-ESI-MS^n analysis.

2.4. Liquid chromatography mass spectrometry

HPLC separations were done on a HP 1100 Series HPLC system. The separations were carried out on a C_{18} RP column (TSKgel ODS-100Z, 150 mm × 4.6 mm ID, 5 μm; Tosoh, Japan) at 35 °C. The mobile phase consisted of ACN and water, with a linear gradient from 30% to 100% ACN in 60 min. The flow rate was 0.8 mL/min and the split ratio to the mass spectrometer was 2:1. The volume injected was 10 μL.

For LC-ESI-MS^n experiments, an Agilent-1100 HPLC system coupled with a LC/MSD Trap XCT ESI mass spectrometer (MA, USA) was employed. The following conditions were applied in all experiments: negative ion mode; collision gas, ultra-high-purity helium (He); nebulizer gas, high-purity nitrogen (N_2), 35 psi; drying gas (N_2), 10 L/min; drying temperature, 350 °C; HV voltage, 4.5 kV; mass range, *m*/*z* 50–1200, compound stability, 100%; trap drive level, 100%; collision energy (Ampl), 30–120%; smart fragmentation, on. Data-dependent MS^n scanning was used in negative ion mode so that the most abundant ions in each MS scan were selected and subjected to ion-trap mass spectrometric (MS^n, n = 2–5) analyses.

2.5. MS^n analysis of standards

The conditions for IT-MS experiments were similar to those for LC-ESI-MS^n experiments. Collision energy (Ampl) was raised until the relative intensity of the precursor ion dropped to approximately 20% (achieved at 40–120%, smart fragmentation, off).

Q-TOF-MS experiments were performed on a Micromass Q-TOF Micro™ (Waters MS Technologies, Manchester, UK), equipped with ESI interface (voltage set to 2.5 kV). The CID mass spectra were recorded under collision energies of 25 V for the investigated compounds; the collision gas argon was at a pressure of 3.0×10^{-5} Torr.

Pure compounds were injected into each spectrometer at a flow rate of 6 μL/min using an external syringe pump.

2.6. NMR

NMR experiments were performed on a Bruker DRX-600 spectrometers (Bruker, Rheinstetten, Germany) equipped with an HX inverse probe (^{1}H: 600 MHz; ^{13}C: 150 MHz). Sample was dissolved in $CDCl_3$ with TMS as internal standard.

3. Results and discussion

Two acetophenones, cynandione A and its derivative, cynandione B, were studied so that the fragmentation patterns of this group could be verified. Fig. 1 shows the structures of the investigated molecules, they contain at least two phenolic hydroxyl groups, which make them predestined for electrospray ionization in negative ion mode.

The product ion spectra of the two acetophenone standards were obtained from the IT instrument and also acquired on the Q-TOF analyzer for further interpreting fragment structures and routes. The results are shown in Figs. 2 and 3. However, there are some obvious differences observed between the MS/MS spectra obtained by the two instruments. The probable reason for the differences from the two MS/MS spectra may be that the ion activation techniques on the Q-TOF and IT instruments are different.

3.1. Fragmentation behavior of cynandione A

Both Q-TOF-MS/MS and ESI-IT-MS/MS spectra of cynandione A are shown in Fig. 2. Although the main fragment peaks occur both in IT-MS/MS and Q-TOF-MS/MS, the spectra look remarkably different (Fig. 2 and Table 1). The fragment ions at *m*/*z* 217, 199, 189, 149 and 109 are only detected in Q-TOF-MS/MS. Fragment ion at *m*/*z*

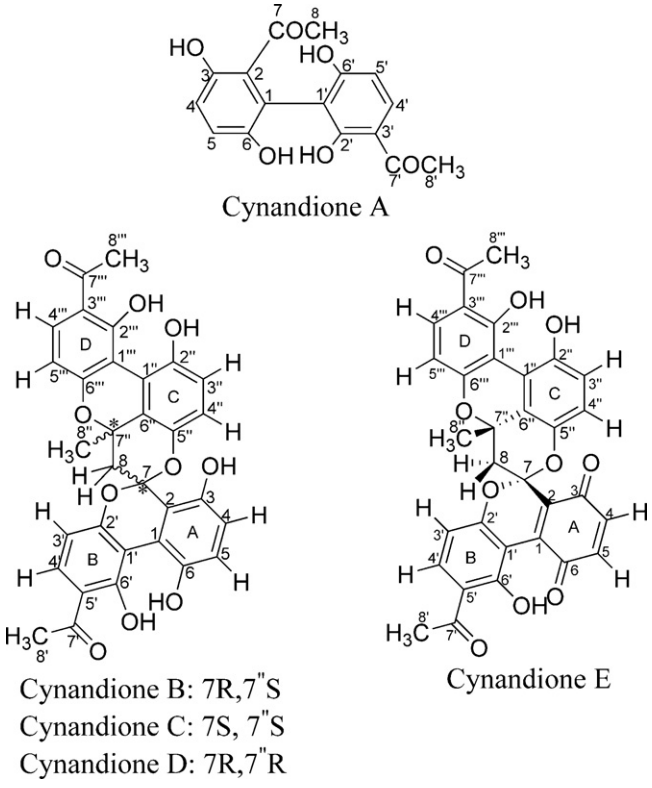

Fig. 1. Structures of investigated compounds.

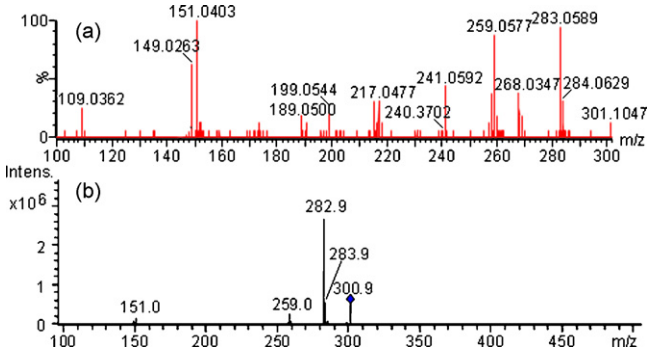

Fig. 2. Negative-ion ESI tandem mass spectra of cynandione A: (a) Q-TOF-MS/MS and (b) IT-MS/MS.

151 represents the base peak in Q-TOF-MS/MS, whereas it is a relatively weak signal in IT-MS[2–5]. Other ions are observed in both types of spectra. Based on these tandem mass spectral data, three main fragmentation pathways of cynandione A are proposed as shown in Scheme 1. Furthermore, these assignments are supported by high-resolution Q-TOF tandem mass measurements and high-resolution MS^2 data of cynandione A together with those of its derivatives which are listed in Table 2.

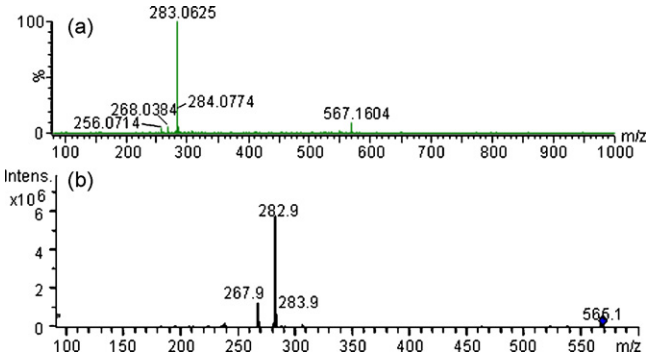

Fig. 3. Negative-ion ESI tandem mass spectra of cynandione B: (a) Q-TOF-MS/MS and (b) IT-MS/MS.

Table 2
Accurate masses and assigned elemental compositions of major fragment ions observed for cynandiones A, B and E.

Compounds	Proposed formula	Measured mass	Calculated mass	Error (ppm)
Cynandione A	$C_{16}H_{11}O_5^-$	283.0589	283.0606	−6.0
	$C_{15}H_8O_5^-$	268.0347	268.0372	−9.3
	$C_{14}H_{11}O_5^-$	259.0577	259.0601	−9.3
	$C_8H_7O_3^-$	151.0403	151.0395	5.3
Cynandione B	$C_{16}H_{11}O_5^-$	283.0625	283.0606	6.7
	$C_{15}H_8O_5^-$	268.0384	268.0372	4.5
	$C_{15}H_{12}O_4^-$	256.0714	256.0736	−8.6
Cynandione E	$C_{18}H_{13}O_6^-$	325.1674	325.1651	7.1
	$C_{18}H_{11}O_5^-$	307.0655	307.0665	−3.2
	$C_{16}H_{11}O_5^-$	283.0597	283.0606	−3.2
	$C_{15}H_8O_5^-$	268.0385	268.0372	4.9

The fragment **a** (m/z 283), arising from the elimination of H_2O from the deprotonated molecule, represents the most prominent fragment ion both in IT and Q-TOF-MS/MS. Therefore, the fragmentation process leading to loss of water molecule (Scheme 1) is the most facile pathway. Such a fragment is found for all investigated acetophenones and plays an important role in further fragmentation pathways (Schemes 1 and 2). Loss of radical methyl group (−15 Da) from ion **a** led to key ion at m/z 268 $[\mathbf{a}-{}^{\bullet}CH_3]^{\bullet-}$, and this fragmentation route was also observed in EI-MS and DCI-MS [7,15,16]. However, the further fragmentation of the $[\mathbf{a}-{}^{\bullet}CH_3]^{\bullet-}$ ion did not present in EI and DCI mass but occur both in IT as well as Q-TOF tandem mass. The product ions at m/z 240 and m/z 225 observed in both types of spectra can be explained by the loss of CO (−28 Da) from $[\mathbf{a}-{}^{\bullet}CH_3]^{\bullet-}$ ion, followed by a methyl radical loss. Additionally, the product ion spectra (Fig. 2) also show that the product ion of m/z 284 (**a**′) due to loss of ${}^{\bullet}OH$ group from $[M-H]^-$ ion was also detected by both instruments. This ion then underwent a similar fragmentation route as that of ion **a** (Scheme 1 and Table 3), yielding the final product ion at m/z 199 due to consecutive losses of ${}^{\bullet}CH_3$ radical, CO and ${}^{\bullet}COCH_2$ group (Scheme 1).

The fragment **b** (m/z 259) with the elemental composition of $[C_{14}H_{11}O_5]^-$ can be interpreted by the loss of an acetyl group (−42 Da) from the $[M-H]^-$ ion. This fragmentation pathway has not

Table 1
ESI-CID-MS/MS of cynandiones A and B in negative mode.

Compound	Precursor ion	Major fragment ions (% of base peak)	
		IT-MS/MS	TOF-MS/MS
Cynandione A	301	301 (41), 284 (16), 283 (100), 259 (21),151 (4)	301 (9), 284 (25), 283 (90), 269 (10), 268 (50), 259 (68), 240 (7), 241 (18), 217 (15), 189 (15), 151 (100), 149 (51), 109 (8)
Cynandione B	567	567 (3), 565 (3), 284 (15), 283 (100), 268 (33)	567 (12), 284 (23), 283 (100), 268 (8), 256 (5)

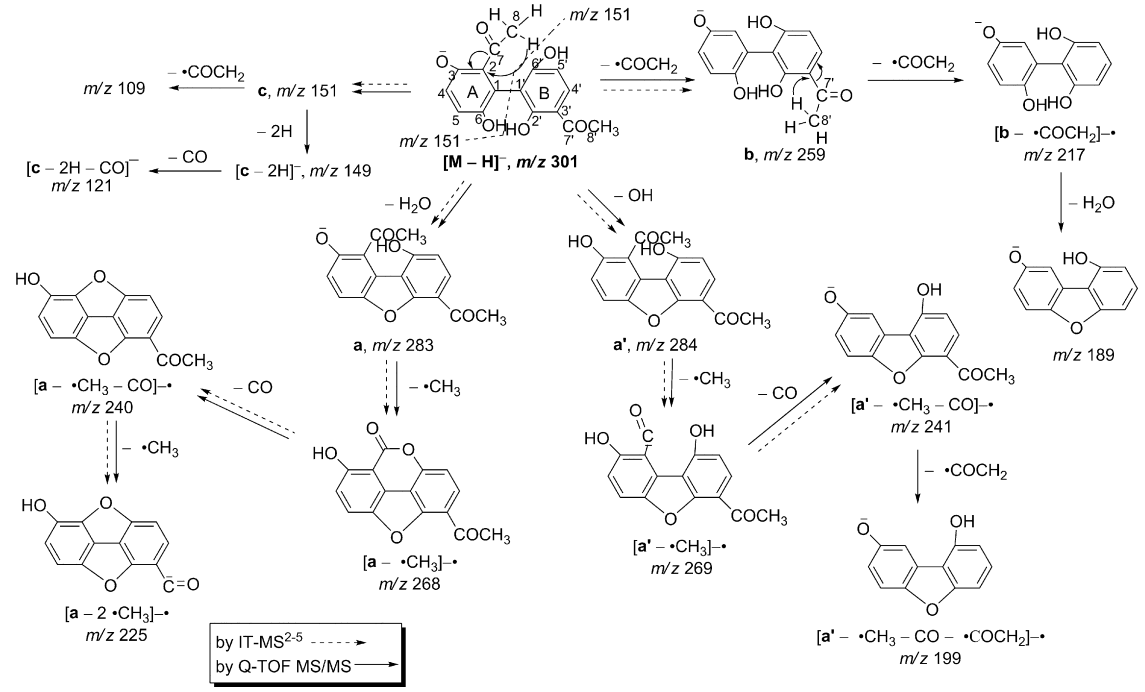

Scheme 1. The proposed fragmentation pathway for cynandione A.

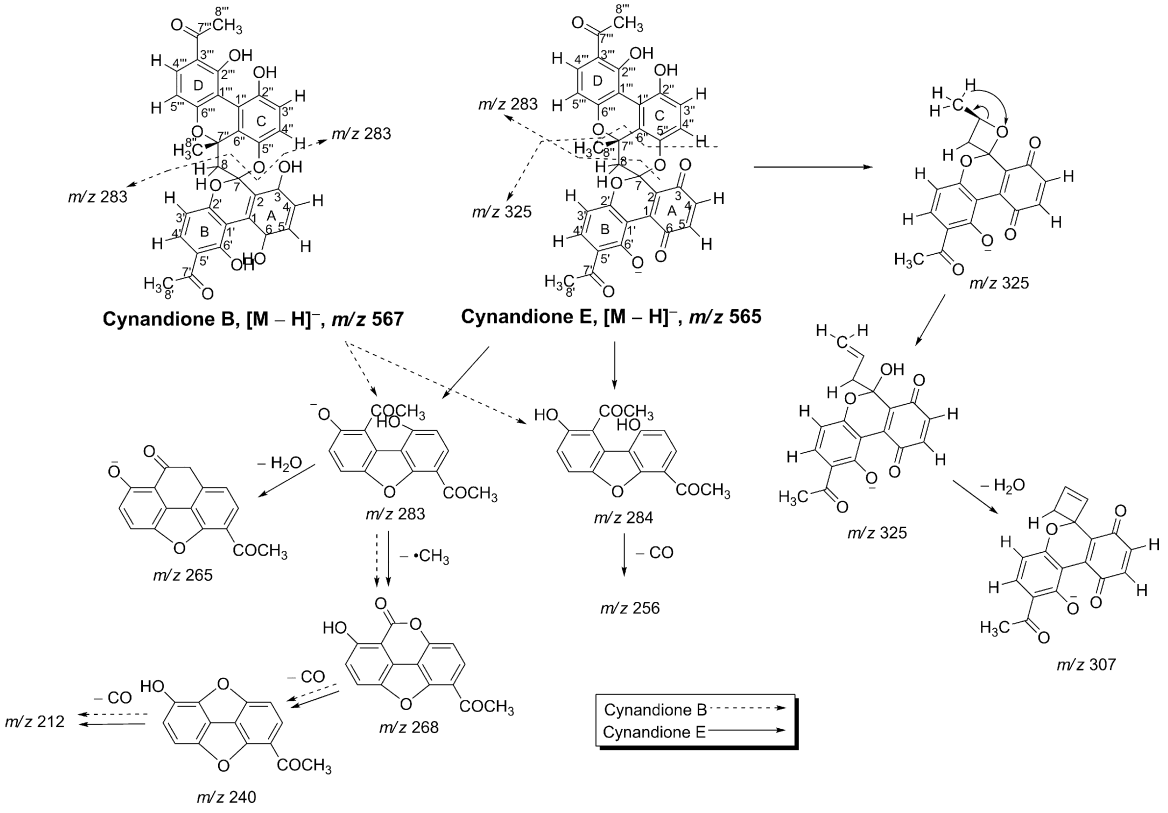

Scheme 2. The proposed fragmentation pathways for both cynandiones B and E.

Table 3
ESI-MS$^{3-5}$ spectral data of cynandiones A and B.

Compound	Major fragment ions (% of base peak)		
	MS^3	MS^4	MS^5
Cynandione A	283 (8), 269 (9), 268 (100)	268 (3), 241 (6), 240 (100)	240 (100), 225 (33)
Cynandione B	283 (17), 269 (10), 268 (100)	268 (90), 240 (100), 225 (9)	240 (100), 212 (90)

been reported previously [8]. The acetyl group loss probably occurs at C_2 position due to α-cleavage followed by H-atom transfer coming from C_8. The ion **b** did not undergo further fragmentation in IT-MS^{2-5}, whereas in Q-TOF CID MS/MS (Fig. 2a), this species gave rise to fragment ions at *m/z* 217 and 189 due to consecutive losses of $^{\bullet}COCH_2$ group and an H_2O molecule, respectively (Scheme 1).

In addition to these general trends, a characteristic fragmentation route, which leads to product ion **c** (*m/z* 151) with the formula $[C_8H_7O_3]^-$, was observed that was probably related to the cleavage of the bridging single C_1—$C_{1'}$ bond between two aromatic rings. It is noteworthy that series fragments resulted from the fragmentation of ion **c** in Q-TOF-MS/MS spectrum such as *m/z* 149 [**c**−2H]$^-$, 121 [**c**−2H−CO]$^-$ and 109 [**c**−$^{\bullet}COCH_2$]$^{\bullet-}$ did not present in IT-MS^{2-5} (Fig. 2 and Table 3). These results can be explained as that the intensity of ion at *m/z* 151 produced in IT-MS/MS was too weak to be further detected for fragmentation. On the contrary, these fragmentation behaviors have not been observed previously [7,15,16].

3.2. Fragmentation behavior of cynandione B

A comparison between the daughter ion spectra of cynandione B obtained using Q-TOF and IT-MS/MS (Fig. 3) shows that almost all the fragments were observed in both spectra (Table 1); the only exception was the ion at *m/z* 256 that was observed only in the Q-TOF-MS/MS spectrum (Fig. 3a) attributed to loss of CO from ion at *m/z* 284 (Scheme 2). However, it is worth noting that, with this one exception, all fragment ions appear in a single ESI-MS/MS spectrum obtained using Q-TOF mass spectrometer, while the same data could be obtained by using the IT in five different and easily interpretable MS^n spectra (Tables 1 and 3).

The prominent fragment ion at *m/z* 283 in both IT and Q-TOF-MS/MS spectra was formed due to dimer cleavage without leaving any functional groups (Scheme 2). This ion then gave the same fragmentation pattern as displayed for cynandione A, and produced the product ions at *m/z* 268 and *m/z* 240. It is worthy of mention that the fragment ion at *m/z* 240 in MS^5 spectrum of cynandione B favored loss of CO to generate product ion at *m/z* 212 (Scheme 2 and Table 3), whereas, the favored fragmentation step of the *m/z* 240 ion in MS^5 spectrum of cynandione A was methyl radical elimination resulting in a strong signal at *m/z* 225 (Scheme 1 and Table 3).

3.3. Identification of acetophenones from C. wilfordii and C. auriculatum

The HPLC-MS chromatograms of standard mixture and both extracts of *C. wilfordii* and *C. auriculatum* are shown in Fig. 4. As mentioned above, the MS^n spectra of cynandiones A and B were dominated by the *m/z* 283 and *m/z* 268 ions, arising from consecutive losses of an H_2O molecule and a methyl group. As shown in Fig. 4c and f, the extraction ion chromatograms (EICs) acquired from extract ion scanning of 283 of the *C. wilfordii* and *C. auriculatum* extracts are similar to the corresponding base peak chromatograms (BPCs) (Fig. 4b and e), but only peaks from acetophenones that derived from cynandione A are observed. In contrast, the signals of the similar peaks in the profiles acquired from extract ion scanning of 268 (Fig. 4d and g) are also similar to corresponding BPCs. Therefore, tandem mass spectrometry with extract ion scanning of 283, in combination with extract ion scanning of 268 that confirms that the compounds are indeed derived from cynandione A, provides a useful means for sensitive detection of acetophenone species derived from cynandione A in mixtures.

As shown in Fig. 4 and Table 4, at least 28 derivatives of cynandione A, including two reference standards, were detected from the root extracts of *C. wilfordii* and *C. auriculatum* by using HPLC-ESI/MS^n method. Among them, only cynandione A has previously been reported from *C. wilfordii* [5]. And other compounds were

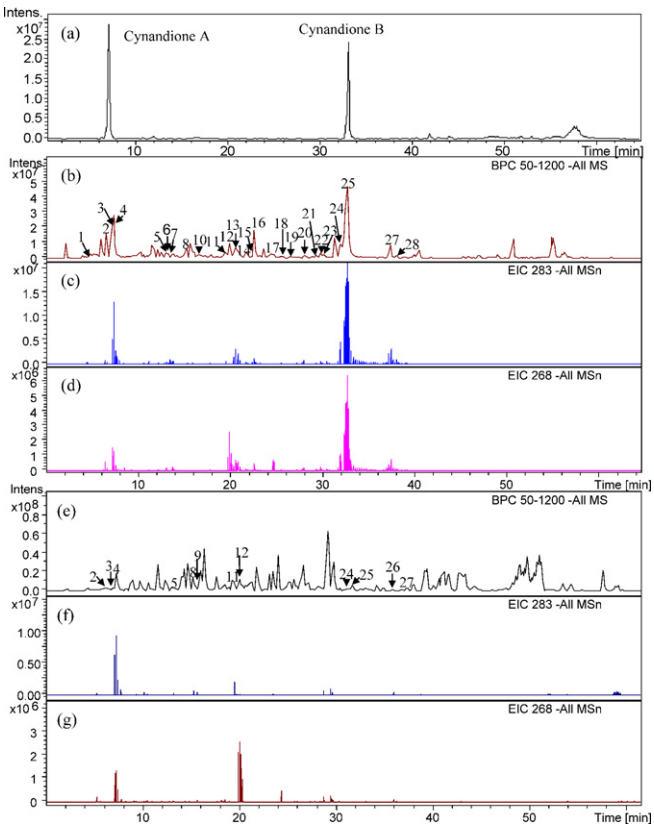

Fig. 4. HPLC-ESI/MS chromatograms in the negative ion mode: (a) base peak chromatogram (BPC) of standards mixture; (b) BPC, (c) extract ion chromatogram (EIC) of 283 and (d) 268 of ethyl acetate extract of *C. wilfordii* roots; (e) BPC, (f) EIC of 283 and (g) 268 of ethyl acetate extract of *C. auriculatum* roots.

reported from this species for the first time and were identified or tentatively characterized based on their tandem mass spectra of the EIC peaks. While for *C. auriculatum*, this study can be considered as the first information on the composition of acetophenones in this species since no previous studies on isolation of acetophenones from *C. auriculatum* has been published. Furthermore, among detected acetophenones, compounds **1**, **6**, **7**, **10**, **13**–**23** and **28** were not detected in *C. auriculatum*, while compounds **9** and **26** were not observed in *C. wilfordii*.

3.3.1. Identification of compounds *2*, *4*, *5*, *10*, *20*, *25* and *26*

4 and **25** represented major acetophenones of the two plants. They could unambiguously be identified as cynandiones A and B, respectively, by comparison of their retention times and MS^n data with those of pure standards (Tables 1, 3 and 4). Compounds **2** and **5** showed similar fragmentation behaviors as for cynandione A, thus were deduced as derivatives of cynandione A. Compound **2** seen with RPLC-ESI-MS eluted ahead of cynandione A and had a molecule weight of 346 amu. Fragmentation pattern and its relative retention suggested that this compound was a carboxyl derivative of cynandione A. Similarly, compound **5** was tentatively characterized as di-cynandione A. In addition, another two minor compounds (**10** and **26**) have similar fragmentation patterns with those of cynandione B. The [M−H]$^-$ ions of them were observed at *m/z* 583 and 551, respectively. The mass difference between each of them and cynandione B is 16 Da, presuming the former has one more hydroxyl group whereas the latter possesses one less hydroxyl group than cynandione B. Accordingly, **10** and **26** were ascribed as hydroxylated and dehydroxylated derivatives of cynandione B, respectively.

Compound **20** exhibited [M−H]$^-$ ion at *m/z* 403, which was 88 Da greater than that of cynanchone A (MW 316) [2,8]. Its MS^{2-4}

Table 4
Identification of acetophenones from the ethyl acetate extracts of *Cynanchum* species.

Peak number	Retention time (min)	Assigned identity	$[M-H]^-$ (m/z)	HPLC/ESI-MS^n (% of base peak)
1	4.4	Cynandione A-*O*-glycoside	463	MS^2[463]: 301 (100), 284 (15), 283 (62), 268 (5) MS^3[463 → 301]: 284 (9), 283 (100), 259 (14); MS^4[463 → 301 → 283]: 268
2	6.4	Carboxyl-cynandione A	345	MS^2[345]: 328 (16), 327 (100), 301 (2), 284 (3), 283 (15) MS^3[345 → 327]: 284 (10), 283 (100), 270 (9), 268 (62) MS^4[345 → 327 → 283]: 268 (59), 241 (100), 193 (6), 181 (6)
3	6.9	Cynandione A-*O*-pentosylglycoside	613	MS^2[613]: 595 (100), 571 (86), 451 (44), 409 (32) MS^3[613 → 595]: 551 (26), 433 (100), 283 (13) MS^4[613 → 595 → 433]: 415 (7), 391 (100), 284 (9), 283 (93), 269 (98), 241 (9), 226 (4), 213 (64)
4	7.3	Cynandione A	301	MS^2[301]: 284 (12), 283 (100), 259 (13), 151 (2) MS^3[301 → 283]: 269 (60), 268 (100), 240 (2); MS^4[301 → 283 → 268]: 241 (5), 240 (100)
5	13.1	Di-cynandione A	601	MS^2[601]: 584 (26), 583 (100), 559 (12) MS^3[601 → 583]: 566 (10), 565 (62), 541 (26), 523 (15), 301 (84), 300 (12), 299 (92), 298 (17), 297 (84), 284 (75), 284 (75), 283 (100), 269 (32), 268 (12) MS^4[601 → 283 → 268]: 268 (100), 241 (83), 228 (12)
6	13.2	Isomer of cynandione B-*O*-pentoside	717	MS^2[717]: 699 (100), 567 (3), 433 (76), 391 (3), 283 (29), 268 (9)
7	13.6	Unknown	557	MS^2[557]: 539 (6), 458 (24), 457 (89), 455 (4), 301 (2), 284 (13), 283 (100), 269 (5), 268 (35) MS^3[557 → 283]: 283 (6), 269 (9), 268 (100), 239 (3) MS^4[557 → 283 → 268]: 240 (100), 225 (37), 212 (24)
8	15.2	Cynandione A-*O*-pentoside	451	MS^2[451]: 434 (22), 433 (100), 409 (37), 300 (3), 299 (19), 255 (2), 151 (2) MS^3[451 → 433]: 418 (100), 298 (14), 297 (14), 283 (13), 269 (9) MS^4[451 → 433 → 418]: 401 (17), 390 (9), 375 (20), 374 (17), 284 (17), 283 (100), 255 (44)
9	15.6	Unknown	527	MS^2[527]: 509 (27), 491 (11), 477 (32), 385 (27), 301 (2), 284 (12), 283 (100), 281 (13), 268 (17) MS^3[527 → 283]: 268 (100), 241 (10), 240 (9), 237 (11)
10	16.5	Hydroxyl-cynandione B	583	MS^2[583]: 566 (6), 565 (11), 556 (28), 555 (100); MS^3[583 → 555]: 513 (100), 445 (32) MS^4[583 → 555 → 513]: 471 (91), 469 (100), 451 (38), 425 (29), 284 (4), 283 (36), 268 (6), 241 (12) MS^5[583 → 555 → 513 → 469]: 451 (19), 427 (100), 425 (87)
11	19.4	Cynandione A-*O*-pentoside	451	MS^2[451]: 433 (100), 409 (31), 301 (3), 283 (4) MS^3[451 → 433]: 418 (9), 415 (4), 298 (25), 297 (46),283 (100), 270 (22), 269 (97), 254 (16), 241 (7) MS^4[451 → 433 → 283]: 254 (100), 241 (12), 239 (10)
12	19.8	Anhydro derivative of cynandione A	283	MS^2[283]: 283 (3), 269 (9), 268 (100), 239 (3) MS^3[283 → 268]: 268 (51), 241 (12), 240 (72), 225 (100), 212 (11)
13	20.5	Chiral isomer of cynandione B	567	MS^2[567]: 284 (17), 283 (100), 269 (5), 268 (22), 241 (2), 240 (5) MS^3[567 → 283]: 283 (9), 269 (9), 268 (100), 239 (2) MS^4[567 → 283 → 268]: 268 (13), 241 (4), 240 (100), 225 (2) MS^5[567 → 283 → 268 → 240]: 184 (100)
14	21.6	Isomer of cynandione B-*O*-pentoside	717	MS^2[717]: 699 (100), 433 (43), 283 (21), 268 (8)

Table 4 (*Continued*)

Peak number	Retention time (min)	Assigned identity	$[M-H]^-$ (*m*/*z*)	HPLC/ESI-MS^n (% of base peak)
15	22.3	Isomer of Cynandione E	565	MS^2[565]: 547 (4), 521 (2), 284 (9), 283 (100), 268 (13) MS^3[565 → 283]: 283 (5), 282 (4), 269 (7), 268 (100), 239 (5)
16	22.5	Isomer of cynandione B-*O*-pentoside	717	MS^2[717]: 699 (100), 433 (4), 283 (11), 268 (4)
17	24.5	Anhydro derivative of cynandione A	283	MS^2[283]: 283 (5), 269 (6), 268 (100), 239 (4) MS^3[283 → 268]: 268 (100), 240 (29), 226 (6), 225 (60), 212 (18), 209 (14) MS^4[283 → 268 → 225]: 197 (100)
18	25.4	Cynandione B-*O*-pentoside	717	MS^2[717]: 699 (79), 433 (100), 283 (33), 268 (9)
19	27.3	Isomer of Cynandione E-*O*-pentoside	715	MS^2[715]: 697 (100), 673 (53), 655 (42), 633 (23), 565 (6), 431 (34), 307 (6), 283 (39), 268 (22), 240 (3)
20	27.9	Dicarboxyl cynanchone A	403	MS^2[403]: 284 (12), 283 (100), 268 (21), 257 (9), 256 (39) MS^3[403 → 283]: 269 (8), 268 (100); MS^4[403 → 283 → 268]: 239 (100)
21	29.2	Cynandione E-*O*-pentoside	715	MS^2[715]: 715 (9), 698 (33), 697 (56), 565 (2), 431 (84), 283 (100), 268 (41) MS^3[715 →]: 268 (100), 239 (2)
22	29.7	Isomer of Cynandione E-*O*-pentoside	715	MS^2[715]: 715 (14), 698 (51), 697 (100), 431 (62), 417 (14), 283 (90), 268 (43), 257 (7), 225 (2)
23	30.4	Chiral isomer of cynandione B	567	MS^2[567]: 284 (11), 283 (100), 269 (4), 268 (20) MS^3[567 → 283]: 283 (5), 269 (4), 268 (100), 239 (3) MS^4[567 → 283 → 268]: 240 (100)
24	31.9	Chiral isomer of cynandione B	567	MS^2[567]: 284 (12), 283 (100), 269 (2), 268 (24), 240 (2) MS^3[567 → 283]: 283 (5), 269 (8), 268 (100), 237 (2) MS^4[567 → 283 → 268]: 268 (2), 241 (2), 240 (100), 225 (12), 212 (2)
25	32.6	Cynandione B	567	MS^2[567]: 284 (12), 283 (100), 269 (2), 268 (25) MS^3[567 → 283]: 283 (5), 269 (9), 268 (100), 239 (2) MS^4[567 → 283 → 268]: 268 (10), 251 (20), 241 (15), 240 (100), 225 (7)
26	37.0	Dehydroxy-cynandione B	551	MS^2[551]: 284 (16), 283 (100), 269 (10), 268 (48) MS^3[551 → 283]: 269 (7), 268 (100), 239 (4)
27	37.3	Cynandione E	565	MS^2[565]: 547 (4), 521 (4), 307 (10), 284 (13), 283 (100), 281 (5), 269 (6), 268 (21) MS^3[565 → 283]: 283 (3), 269 (12), 268 (100), 239 (4) MS^4[565 → 283 → 268]: 268 (71), 240 (53), 225 (100)
28	38.0	Isomer of Cynandione E	565	MS^2[565]: 547 (4), 521 (3), 307 (7), 284 (11), 283 (100), 281 (5), 269 (3), 268 (16) MS^3[565 → 283]: 283 (6), 282 (3), 269 (5), 268 (100), 239 (3); MS^4[565 → 283 → 268]: 225 (100)

spectra gave a list of abundant ions at *m*/*z* 283, 268 and 239, which were obviously the characteristic ions of both cynandione A and cynanchone A [8]. Thus compound **20** should possess two more carboxyl groups than cynanchone A. Hence, compound **20** was tentatively identified as dicarboxyl cynanchone A.

3.3.2. *Differentiation of isomers **12**, **13**, **15**, **17**, **23**, **24**, **25**, **27** and **28***

Two compounds (**12** and **17**) in both BPC and EIC exhibited $[M-H]^-$ ions at *m*/*z* 283, a decrease of 18 Da than that of cynandione A. Their MS^2 and MS^3 spectra are almost the same, which gave prominent ions of *m*/*z* 268, *m*/*z* 240 and *m*/*z* 225 (Table 4), consistent with the major fragmentation pathway of cynandione A. Using this information together with the differences of molecular weights between each of them and cynandione A, we present proposals for identifications of these two new acetophenones, i.e., anhydro derivatives of cynandione A. One of them may be produced by the dehydrolysis reaction between C_6—OH and $C_{2'}$—OH on the structure of cynandione A, forming a stable structure as shown in Scheme 1**a**, and the other is most probably its positional isomer.

In addition, three chiral isomers of cynandiones B, C and D were isolated from *C. taiwanianum* [8], and their absolute configurations were assigned as 7R; 7″S, 7S; 7″S and 7R; 7″R, respectively [17]. However, the structure of cynandione B bears two chiral centres (Scheme 2), it should thus give rise to four possible stereoisomers that exist as two pairs of geometric isomers. In this study, the EIC

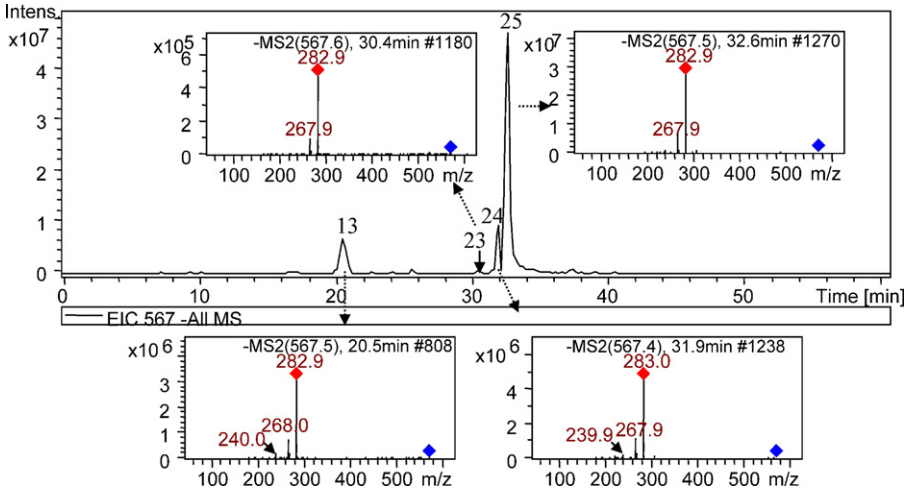

Fig. 5. Extract ion chromatogram (EIC) scanning of *m*/*z* 567.

scanning for the parent ion at *m*/*z* 567 revealed four peaks eluting at 20.5 min (**13**), 30.4 min (**23**), 31.9 min (**24**) and 32.6 min (**25**) with similar fragmentation patterns (Fig. 5), suggesting that cynandione B and its chiral isomers coexist in *C. wilfordii*.

Meanwhile, product-ion analysis showed three isomeric structures for the ions at *m*/*z* 565 eluting from 22.3 min (**15**), 37.3 min (**27**) and 38.0 min (**28**), respectively. The major ions obtained in MS^{2-5} spectra of these three compounds were similar to those of cynandione B (Table 4), even though a decrease of 2 Da when compared to the molecular weight of cynandione B. Based on the above evidences, **15**, **27** and **28** were deduced as the oxidation derivatives of cynandione B. The oxidation reaction may occur at phenol hydroxyl groups. However, there are five phenol hydroxyl groups in the structure of cynandione B. The oxidation reactions at $C_{6'}$—OH, $C_{2''}$—OH and $C_{2'''}$—OH may not easily occur due to generating compounds of olefine ketone (—C=C=O) which are labile. Therefore, C_3—OH and C_6—OH may be the most favorable positions for the oxidation reaction to form *para*-benzoquinone which is relatively stable. The outlined structure for these compounds could be assigned as shown in Fig. 1.

The product ion spectra of the $[M-H]^-$ ions of above-mentioned compounds did not show any fragmentation patterns which, upon visual inspection, allowed isomeric compounds to be differentiated. Therefore, we attempt to discriminate these isomers via the breakdown curves constructed by collision energy versus relative intensity of selected fragment ions. Through evaluating breakdown curves, information on fragmentation mechanisms such as identification of isomers and tautomers; distinguishing between competitive and consecutive fragmentation pathways as well as the stability of product ions, can be obtained [18–21].

12 and **17** were ascribed as positional isomers and their breakdown curves are shown in Fig. 6. The fragment ion at *m*/*z* 239 by loss of 44 Da ($-{}^{\bullet}C_2H_4O$) from precursor ion $[M-H]^-$ at *m*/*z* 283 was minor peak in MS^2 spectrum of each compound. However, the curves for the formation of the ion at *m*/*z* 239 for these two compounds showed different shapes and appearance energies which indicated they were formed by different mechanism. Meanwhile, collisional spectra put in evidence that ${}^{\bullet}C_2H_4O$ group loss was energetically more favorable for compound **17**. In fact, the energy for the formation of the *m*/*z* 239 ion with highest relative abundance was at 0.4 V for **17** and 0.9 V for **12**. Consequently, it is proposed that these two positional isomers can be differentiated by their breakdown curves.

The breakdown curves of **13**, **23**, **24** and **25** (Fig. 6) were also investigated with little differences observed. These four compounds produced two fragment ions in MS^2 experiment except for the base peak at *m*/*z* 283. Although in low intensities, the *m*/*z* 284 and 263 ions for **13**, **23**, **24** and **25** displayed different breakdown curves. Breakdown curves of the former two compounds showed the different shapes and appearance energies in low collision energy regions (0.2–0.4 V). The latter two also presented similar phenomena. Whereas at increasingly higher energies (0.5–1.2 V), curves for **13** and **25** possessed similar breakdown potential. However, the breakdown curves for **13** and **24** are remarkably different, similar phenomena were presented in **23** and **24** as well as in **23** and **25**. Therefore, it can be deduced that the breakdown curves were useful for differentiation of these four chiral isomers. Similar observations were made for isomers **15**, **27** and **28**. Accordingly, these three compounds might be deduced as the stereochemical isomers, with stereochemical differences in C_7 and $C_{7''}$ positions. However, the exact structures of these compounds and differentiation of chiral isomers via the relationships between breakdown curves need further investigations.

3.3.3. *Identification of O-glycosides **1**, **3**, **6**, **8**, **11**, **14**, **16**, **18**, **19**, **21** and **22***

Previous studies on some *Cynanchum* species have shown the presence of acetophenone hexosides [22]. The aglycones included two isomers, 2,4-dihydroxyacetophenone and 3,4-dihydroxyacetophenone, the sugar moieties belong to glucose. In the present study, HPLC-ESI-MS^n analysis of the extracts also showed five glycosylated acetophenones in the two investigated *Cynanchum* species. Among them, compounds **1**, **3**, **8** and **11** bear the same aglycone which exhibited the same fragmentation pattern as that of cynandione A. For compound **3**, consecutive loss of a hexose (glucose or galactose) (−162 Da) and a pentose (arabinose, xylose or lyxose) residue with retention of the glycosidic oxygen atom (−150 Da), was detected. Fragment ion at *m*/*z* 451, by loss of 162 Da from deprotonated ion at *m*/*z* 613, suggested the terminal glucose residue. Consequently, the disaccharide sequence of **3** was hexose–pentose–(*m*/*z* 613 → 451 → 433 → 283). Based on the fragmentation behaviors and literature data, **3** was tentatively identified as cynandione A-*O*-pentosylglucoside. Similarly, **1** was assigned as cynandione A-*O*-glucoside, and another two compounds (**8** and **11**) with $[M-H]^-$ ion at *m*/*z* 451 were tentatively identified as cynandione A-*O*-pentosides. Breakdown curves of the *m*/*z* 409 ion for **8** and **11** (Fig. 6) displayed different shapes and appearance energies indicating that these two isomers can be promptly discriminated by breakdown curves. The higher relative intensity of the *m*/*z* 409 ion

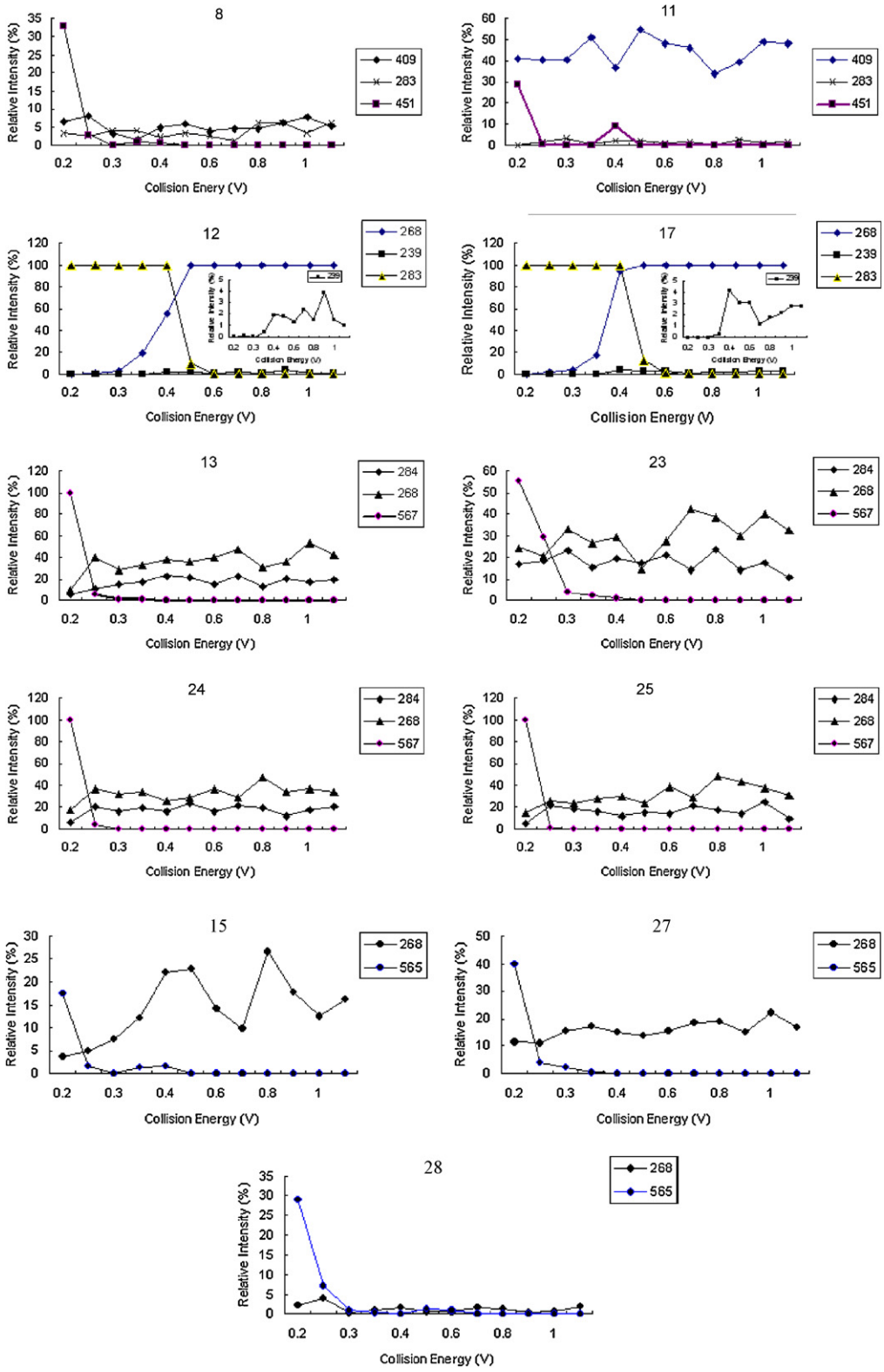

Fig. 6. Breakdown curves of MS^2 ions of compounds **8**, **11**, **12**, **13**, **15**, **17**, **23**–**25**, **27** and **28**.

showed that **11** fragmented to lose $COCH_2$ group more easily than **8** did.

In the same way, four compounds (**6**, **14**, **16** and **18**) exhibiting $[M-H]^-$ ion at *m*/*z* 717 were tentatively identified as *O*-pentosides of compounds **13**, **23**, **24** and cynandione B (**25**), respectively, on the basis of their similar fragmentation characteristics and elution orders. Similarly, **19**, **21** and **22** with deprotonated ion at *m*/*z* 715 were ascribed as *O*-pentosides of **15**, cynandione E (**27**) and **28**, respectively.

3.3.4. *Identification of* **7** *and* **9**

Both compounds **7** and **9** have similar fragmentation patterns. The $[M-H]^-$ ions of them were observed at *m*/*z* 557 and 527, respectively. The mass difference between **7** and **9** is 30 Da, presuming

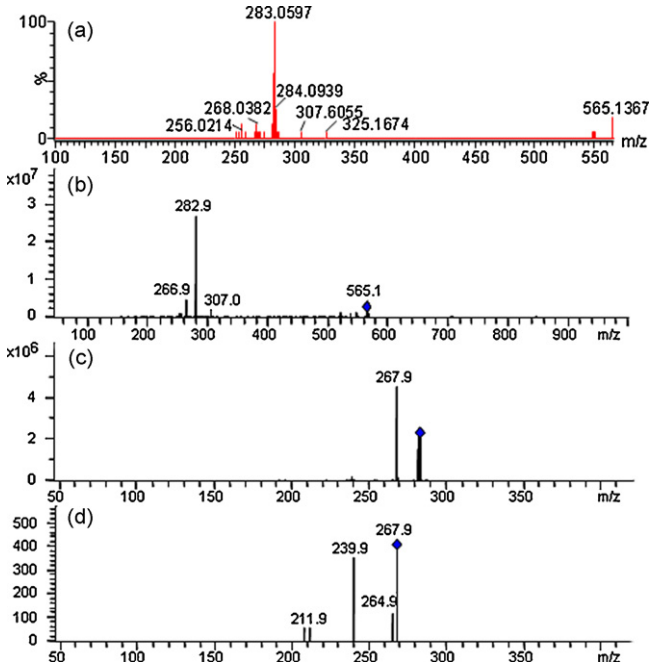

Fig. 7. Negative-ion ESI-MS^n spectra of cynandione E acquired on the both Q-TOF and IT instruments: (a) Q-TOF-MS/MS, (b) IT-MS^2, (c) IT-MS^3 and (d) IT-MS^4.

that **7** have one more methyloxyl group. These two compounds underwent fragmentation processes consistent with cynandione A, suggesting that **7** and **9** are derivatives of cynandione A. However, MS^n experiments did not provide more efficient information to help elucidate their structures and their exact structures need to be confirmed by NMR in the future study.

3.4. Isolation and structure determination of compound **27**

To confirm the accuracy of the assignment procedure, the most abundant novel compound **27** was isolated and characterized by NMR (see Supplementary Material for ^{1}H and ^{13}C resonances). The ^{1}H NMR spectral data suggested that compound **27** is a tetraacetophenone derivative. The ^{1}H and ^{13}C NMR spectra of compound **27** showed similar chemical shifts to those of cynandione B [9], except that C_1–C_6 of A ring exhibited significant downfield shifts which indicated a *para*-benzoquinone ring. The HMBC spectrum of **27** (see Supplementary data) showed similar correlations of ring A–D to that of cynandione B. Based on a theory of long-range heteronuclear coupling constants of H^1 and C^{13} [23], HMBC experiments and the vicinal coupling constants of ^{1}H–^{13}C correlations were applied to determine the relative stereochemistry of **27**. The novel compound **27** was assigned as cynandione E, which was emphasized by structural information obtained from IT-MS$^{2-4}$ and Q-TOF-MS/MS (Fig. 7). As can be seen from Fig. 7, the $[M-H]^-$ ion at m/z 565 showed similar fragmentation patterns to those of cynandione B, except for ions of m/z 325, 307 and 265. The fragmentation routes proposed for the prominent ion at m/z 283 agree with evidence from MS^3 and MS^4 experiments of cynandione B, showing that the m/z 283 ion has the same structure as that produced by $[M-H]^-$ ion of cynandione B (Scheme 2). The origin of m/z 325 ion was presumed to be generated by the bond cleavages of $C_{5''}$—O, $C_{6''}$—$C_{7''}$ and $C_{7''}$—O, leading to the specific fragment ion as shown in Scheme 2. This ion further underwent to loss of water molecule to produce fragment ion at m/z 307. The generation of the product ion at m/z 265 was proposed as loss of water from the m/z 283 ion, and the fragment ion at the m/z 256 producing in Q-TOF-MS/MS spectrum corresponded to CO loss from the m/z 284 ion. Most of above-mentioned assignment were consistent with those supposed by high-resolution Q-TOF tandem mass measurements (Table 2). The above results showed that although the stereochemical information of the compounds was not available by MS, the structural information can be extracted from the MS spectra and proposals can be given.

4. Conclusions

The Q-TOF-MS/MS and IT-MS^n analysis in the present study revealed that the major fragmentation reactions of the investigated acetophenones consist of elimination of water, methyl radical and CO as well as dimer cleavage. For cynandiones A and B, the ions at m/z 283 and m/z 268 are the diagnostic fragment ions, which could be used to detect derivatives of cynandione A in *Cynanchum* species in combination with tandem mass spectral rules. Based on these indicative data, total of 28 cynandione A derivatives were identified or tentatively characterized from the EtOAc extracts of *C. wilfordii* and *C. auriculatum* roots. Among them, a new tetraacetophenone was isolated and named cynandione E based on analysis of its mass spectral data, NMR spectroscopic and NOE spectra. Furthermore, positional isomers and chiral isomers investigated in this study can be differentiated promptly by evaluation of their breakdown curves, though each group of them yields the same product ions. Hence, the proposed HPLC-ESI-MS^n method is simple and efficient for rapidly screening and identifying cynandione A derivatives in complex mixtures.

Acknowledgments

This work was supported by program for Changjiang Scholars and Innovative Research Team in University (PCSIRT), NCET Foundation, NSFC (30725045), National 863 Program (2006AA02Z338), Shanghai Leading Academic Discipline Project (B906) and in part by the Scientific Foundation of Shanghai China (07DZ19728, 06DZ19717, 06DZ19005).

Appendix A. Supplementary data

Supplementary data associated with this article can be found, in the online version, at doi:10.1016/j.jpba.2009.01.009.

References

[1] Z.Y. Wu, L.G. Fu, Flora Reipuβlicae Popularis Sinicae, Science Press, Beijing, 1977, pp. 249–310.
[2] B.Y. Hwang, Y.H. Kim, J.S. Ro, K.S. Lee, J.J. Lee, Arch. Pharm. Res. 22 (1999) 72–74.
[3] B.Y. Hwang, S.E. Kim, Y.H. Kim, H.S. Kim, Y.S. Hong, J.S. Ro, K.S. Lee, J.J. Lee, J. Nat. Prod. 62 (1999) 640–643.
[4] D.U. Lee, U.S. Shin, K. Huh, Planta Med. 62 (1996) 485–487.
[5] M.K. Lee, H.S. Yeo, J.W. Kim, G.J. Markelonis, T.H. Oh, Y.C. Kim, J. Neurosci. Res. 59 (2000) 259–264.
[6] M.K. Lee, H.S. Yeo, J.W. Kim, Y.C. Kim, J. Pharm. Pharmacol. 52 (2000) 341–345.
[7] P.L. Huang, S.J. Won, S. Hwa Day, C.N. Lin, Helv. Chim. Acta 82 (1999) 1716–1720.
[8] C.N. Lin, P.L. Huang, C.M. Lin, M.H. Yen, R.R. Wu, Phytochemistry 44 (1997) 1359–1363.
[9] Y.L. Lin, Y.M. Wu, Y.H. Kuo, Phytochemistry 45 (1997) 1057–1061.
[10] X.J. Cao, Y.P. Tai, X.Y. Li, Y.P. Ye, Y.J. Pan, Rapid Commun. Mass Spectrom. 39 (2004) 691–701.
[11] R. Li, Y. Zhou, Z.J. Wu, L.S. Ding, J. Mass Spectrom. 41 (2006), 1–C22.
[12] L.M. Souza, T.R. Cipriani, M. Iacomini, P.A.J. Gorin, G.L. Sassaki, J. Pharm. Biomed. Anal. 47 (2008) 59–67.
[13] J.J. Chen, Y.P. Ye, C.R. Sun, Y.J. Pan, Anal. Chim. Acta 613 (2008) 74–82.
[14] M. Yin, X. Feng, Y.F. Dong, C.Q. Yuan, Chin. Wild Plant Resour. 23 (2004) 8–11.
[15] P.L. Huang, C.M. Lu, M.H. Yen, R.R. Wu, C.N. Lin, Phytochemistry 40 (1995) 537–541.
[16] P.L. Huang, C.M. Lu, M.H. Yen, R.R. Wu, C.N. Lin, Phytochemistry 41 (1996) 293–295.
[17] C.C. Lin, P.L. Huang, J.J. Wang, S.H. Day, H.C. Lin, J.P. Wang, Y.L. Ko, C.M. Teng, Biochim. Biophys. Acta 1380 (1998) 115–122.

[18] P.J. Dyson, B.F.G. Johnson, J.S. McIndoe, P.R.R. Langridge-Smith, Rapid Commun. Mass Spectrom. 14 (2000) 311–313.
[19] A.G. Harrison, J. Mass Spectrom. 34 (1999) 1253–1273.
[20] M. Begala, G. Delogu, E. Maccioni, G. Podda, G. Tocco, E. Quezada, E. Uriarte, M.A. Fedrigo, D. Favretto, P. Traldi, Rapid Commun. Mass Spectrom. 15 (2001) 1000–1010.
[21] H.I. Kenttamaa, R.G. Cooks, J. Am. Chem. Soc. 107 (1985) 1881–1886.
[22] Y.L. Lin, T.C. Lin, J. Nat. Prod. 60 (1997) 368–370.
[23] Horst Kessler, C. Mesinger, K Wagner, J. Am. Chem. Soc. 109 (1987) 6927–6933.